ACS OMEGA

Open Access

http://pubs.acs.org/journal/acsodf

Article

Effects of Temperature on Novel Molecular Perovskite Energetic Material $(C_6H_{14}N_2)[NH_4(ClO_4)_3]$: A Molecular Dynamics Simulation

Qiaoli Li,[†] Shenshen Li,[†] and Jijun Xiao*

Cite This: *ACS Omega* 2024, 9, 4013−4018

Read Online

ACCESS | Metrics & More | Article Recommendations

ABSTRACT: Molecular dynamics (MD) simulations were performed on the energetic molecular perovskite $(C_6H_{14}N_2)[NH_4(ClO_4)_3]$, with excellent detonation properties, thermal stability, and high specific impulse, which is a potential replacement for AP as the next generation propellants. The cohesive energy density, binding energy, pair correlation function, maximum bond length (L_{max}) of the N−H trigger bond, and mechanical properties of the $(C_6H_{14}N_2)[NH_4(ClO_4)_3]$ were reported. The calculated cohesive energy density and binding energy decrease with increasing temperature, indicating a gradual decrease in the thermal stability with temperature. In addition, H···O hydrogen bonding interactions have been found based on the results of pairwise correlation functions. The maximum length (L_{max}) of the N−H trigger bond was calculated and used as a criterion to theoretically judge the impact sensitivity. The maximum bond length of the N−H trigger bond grows gradually with temperature; however, it does very slightly yet gradually above 373 K. This suggests that an increase in temperature leads to a higher impact sensitivity and lower thermal stability. However, this effect becomes less pronounced when the temperature surpasses 373 K. Moreover, the calculated mechanical data indicate that as the temperature rises, the material's stiffness, hardness, yield strength, and fracture strength all decrease. The material's ductility shows an upward trend with increasing temperature, reaching its peak at 373 K and subsequently declining as the temperature continues to rise.

1. INTRODUCTION

Perovskite materials have gained considerable attention as a hot research area in solar cells,[1,2] ferroelectrics,[3] detectors,[4] and other domains due to their distinct structures and exceptional capabilities. Recently, a series of molecular perovskite compounds with high-energetic, known as DAPs, have been created and synthesized by Chen's team,[5−8] which marks the beginning of the application of perovskite in high-energetic materials. Different from traditional energetic materials, these energetic molecular perovskites have unique structure features where the inorganic oxidizer components and organic fuel are tightly packed at the molecular level into a highly symmetric ternary unit. The unique structural features make these energetic molecular perovskites possess excellent thermal stabilities, superior detonation performances, and low cost.

Among these energetic molecular perovskites, the compound $(C_6H_{14}N_2)[NH_4(ClO_4)_3]$ DAP-4 exhibits outstanding comprehensive performances (detonation velocity D = 8806 m s^{-1}; detonation pressure P = 35.2 GPa; thermal decomposition temperature T_d = 358 °C),[9] which are higher than those of RDX (D = 8634 m s^{-1}, P = 33.3 GPa, T_d = 210 °C)[9] and comparable to HMX (D = 8892 m s^{-1}, P = 36.2 GPa, T_d = 279 °C).[9] More remarkably, it exhibits an extremely high specific impulse (I_{sp} = 254 s) much higher than that of ammonium perchlorate (AP) (I_{sp} = 157 s), the most-commonly used oxidizing component in solid rocket.[5] Moreover, DAP-4 synthesized from AP using a molecular assembly strategy has a good oxygen supply capacity. Therefore, DAP-4 is being given more and more consideration as a potential alternative for AP in high-energy composite solid rocket propellants,[10] thereby attracting the attention of a growing number of researchers. By combining differential scanning calorimetry (DSC) and simultaneous thermal analysis methods to investigate the thermal behaviors of DAP-4, Zhou et al.[11] pointed out that the first thermal decomposition stage occurred with the proton transfer from organic cations H_2dabco^{2+} and NH_4^+ to ClO_4^- to form NH_3 and $HClO_4$ when the temperature was higher than 370 °C. Deng et al.[12] reached the same conclusion by studying the thermal decomposition of DAP-4. Besides, there are many studies on the thermal decomposition of DAP-4 by using catalysis such as MoS_2 nanosheets, Ti_3C_2 MXene, and so on.[13−17]

Despite the fact that there are many studies on DAP-4 today, the majority of these studies mainly focus on thermal decomposition using experimental methods, and a theoretical study on DAP-4 is still blank. In order to gain a deeper and more systematic understanding of DAP-4, molecular dynamics (MD) simulations of DAP-4 at different temperatures were carried out in this paper. In our work, the variations of cohesive energy density (CED) and binding energy (E_{bind}) with temperature were provided and correlated with thermal

Received: November 3, 2023
Revised: December 11, 2023
Accepted: December 15, 2023
Published: January 5, 2024

Table 1. Lattice Constants and Density of DAP-4 Crystal by MD and Experiment[a]

methods	a (Å)	b (Å)	c (Å)	α (deg)	β (deg)	γ (deg)	ρ (g/cm^3)
Expt	14.426	14.426	14.426	90.0	90.0	90.0	1.87
NPT	14.467	14.447	14.359	90.0	90.2	90.1	1.89
	(+0.28%)	(+0.15%)	(−0.46%)	(0%)	(+0.22%)	(+0.11%)	(+1.07%)

[a]The corresponding deviations are given in parentheses.

stability of the crystal. The pair correlation function (PCF) was applied to investigate the interactions between the different ions. Particularly, the N−H trigger bond lengths of DAP-4 were discussed in terms of the relationship with sensitivity. Besides, the mechanical properties at different temperatures, including the tensile modulus (E), bulk modulus (K), shear modulus (G), Poisson's ratio (ν), and Pugh's ratio (K/G), were also calculated and discussed in this work.

2. COMPUTATIONAL METHODS

All MD simulations were performed using a modified pcff force field developed by Zhu's teams,[18] which is an all-atom force field for ammonium perchlorate (AP) and has been successfully applied to MD simulations of AP/HMX composite. For simplicity, this force field was abbreviated as the pcff-AP force field in this work. On the basis of the crystal parameters obtained from X-ray diffraction,[5] a supercell composed of 2 × 2 × 2 unit cells was constructed. Each cell contained a total of 64 $(C_6H_{14}N_2)[NH_4(ClO_4)_3]$ molecules and 2688 atoms. All the models were allowed to evolve dynamically in isothermal−isobaric (NPT) ensemble, where the temperature was maintained using the Andersen stochastic collision method[19] and the pressure was managed using the Parrinello−Rahman[20] scheme with all cell parameters fully relaxed at atmospheric pressure. The cell time constant used to control the pressure was set at 1.0 ps. The temperature started from 223 to 423 K in step of 50 K. The van der Waals (vdW) interactions were truncated at 12.5 Å with long-range tail correction[21] and the electrostatic interactions were calculated via the standard Ewald summation.[22] The equations of motion were integrated with a step of 0.5 fs, and the equilibration run was performed for 5 ns. After the equilibration run, production runs of 1 ns were performed, during which data were collected with 10 fs sampling interval for analysis. These calculations were all performed using the software Material Studio from Biovia Inc.

3. RESULTS AND DISCUSSION

To validate the applicability of the pcff-AP force field parameters to DAP-4 crystal, the cell parameters and density were calculated and compared with experimental values. The calculations were conducted with full relaxation of all cell dimensions and angle parameters without any symmetry constraints (P1 space group). The simulated data for cell parameters and densities as well as experimental data[5] are tabulated in Table 1. It is clear that the pcff-AP force field gives a good and accurate reproduction of the experimental values for lattice constants. The densities were calculated only with an error of 1.07%. The unit cell structure and the equilibrium supercell structure of DAP-4 are displayed in Figure 1.

3.1. Cohesive Energy Density. The cohesive energy density (CED) is the quantity of energy required to totally separate molecules from one another per mole for unit volume until there are no interactions within or the energy required to transition from the condensed phase to the gas phase per mole for unit volume. In atomistic simulations, cohesive energy corresponds to the increase in energy when all intermolecular forces per mole of a material are vanished, and the CED is defined as per unit volume of which.

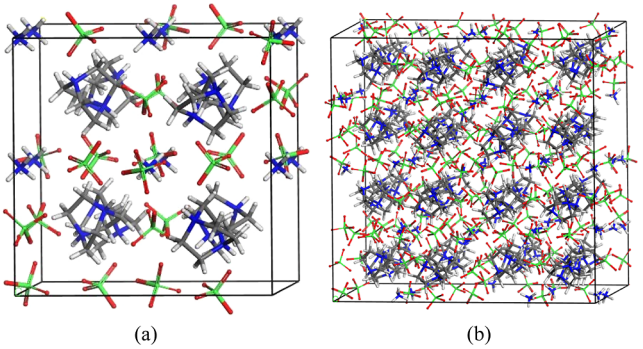

Figure 1. (a) Unit cell structure of DAP-4; (b) equilibrium supercell structure of DAP-4. H atom in light gray, C atom in dark gray, N atom in blue, O atom in red, and Cl atom in green.

The CEDs of DAP-4 at different temperatures are displayed in Table 2. As seen in Table 2, CED is the sum of vdW and electrostatic energy under the pcff-AP force field. It is also can be found that the cohesive energy density primarily comes from electrostatic interactions. Additionally, it is clear that the CED, vdW, and electrostatic energy in DAP-4 decrease monotonically with increasing temperature. Accordingly, the energy needed to transition a material from its condensed phase to the gas phase, where it is more likely to decompose and explode, would drop as temperature rose. Therefore, it is conceivable that when temperature rises, DAP-4's thermal stability declines and its sensitivity rises as a result.

3.2. Binding Energy. The binding energy (E_{bind}), which can reflect how well the components are blended with one another, is characterized as having a negative value as the intermolecular interaction energy. By subtracting the energy of individual component from the total energy of the entire system, one can compute the energy of intermolecular interactions between various components.[23] For the ABX_3-type molecular perovskite $(C_6H_{14}N_2)[NH_4(ClO_4)_3]$, $C_6H_{14}N_2^{2+}$, NH_4^+, and ClO_4^- denote the A-site, B-site, and X-site ions, respectively. As mentioned above, the E_{bind} of DAP-4 can be expressed as follows

$$E_{bind} = -E_{inter} = -(E_{total} - E_A - E_B - E_X)$$

where E_{total} represents the total energy of the whole system, E_A, E_B, and E_X are the energies of A-site, B-site, and X-site ions, respectively. The total energies (E_{total}) of the whole system, the energies of A, B, and X ions, and the binding energies (E_{bind}) of the DAP-4 crystal at different temperatures are tabulated in Table 3.

The binding energy denotes the degree of interaction among the different components and can reflect the thermal stability of the system.[24] A higher binding energy indicates a stronger

https://doi.org/10.1021/acsomega.3c08711
ACS Omega 2024, 9, 4013−4018

Table 2. Cohesive Energy Density CED, vdW, and Electrostatic Energy of DAP-4 at Different Temperatures (kJ cm^{-3})

	temperature/K				
energy	223	273	323	373	423
CED	3.77(0.02)	3.65(0.02)	3.48(0.01)	3.37(0.01)	3.26(0.02)
Vdw	0.58(0.00)	0.56(0.00)	0.51(0.01)	0.48(0.00)	0.45(0.01)
Electrostatic	3.19(0.00)	3.09(0.01)	2.97(0.01)	2.89(0.01)	2.81(0.01)

Table 3. E_{total}, E_A, E_B, E_X, and E_{bind} of DAP-4 at Different Temperatures (kJ mol^{-1})[a]

T/K	E_{total}	E_A	E_B	E_X	E_{bind}
223	−9310.8(26.2)	−4032.5(18.3)	−1840.5(8.4)	−313.2(13.5)	3124.7(12.7)
273	−8860.9(30.3)	−3789.6(21.5)	−1799.2(10.4)	−195.3(17.7)	3076.8(14.2)
323	−8336.8(34.9)	−3521.0(25.0)	−1749.7(14.8)	−75.6(19.1)	2990.6(13.6)
373	−7881.1(38.4)	−3279.9(37.0)	−1701.6(12.5)	39.4(22.4)	2939.1(16.5)
423	−7438.4(45.8)	−3042.6(37.0)	−1655.0(16.0)	147.6(30.1)	2888.4(18.9)

[a]The corresponding deviations are listed in parentheses.

interaction between the components and therefore a more stable system. It is clearly seen that the E_{bind} value of the compounds gradually decreases with an increase in temperature, which demonstrates that the thermodynamic stability of the system decreases. This conclusion echoes that of obtained from cohesive energy density. Additionally, it can be found that the value of E_X increased with temperature and became positive when the temperature was higher than 373 K. Therefore, it might be roughly speculated that this compound would begin to become unstable at this temperature.

The breakdown of E_{bind} is seen in Table 4. It is discovered that electrostatic interactions, which account for around 65%

Table 4. Decomposed Components of $E_{binding}$ at Different Temperature (kJ/mol)[a]

T/K	E_{bind}	E_{vdw}	$E_{electro}$
223	3124.7(12.7)	1083.7(13.8)	2041.0(9.1)
273	3076.8(14.2)	1072.9(14.9)	2003.8(8.7)
323	2990.6(13.6)	998.7(16.0)	1991.9(12.0)
373	2939.1(16.5)	957.6(18.2)	1981.5(9.5)
423	2888.4(18.9)	925.0(17.6)	1963.4(10.3)

[a]The corresponding deviations are listed in parentheses.

of E_{bind}, are the dominant source of binding energy. This implies that there are strong electrostatic interactions among these ions. Furthermore, it can be observed that the absolute value of electrostatic energy is greater than that of vdW energy; hence, we may infer that the electrostatic interactions play a crucial part in the molecular interactions among different ions. This is mainly due to the characteristics of the unique perovskite where exist the alternately packed cations and anions amounts of charges.

3.3. Pair Correlation Function Analysis. The pair correlation function (PCF) is a useful and practical physical tool as it can give insight into the structure of a material by measuring the local spatial ordering and thus the probability density $g(r)$ of finding an atom at a distance from a reference atom. In general, the distance range for hydrogen bonds is 2.0−3.1 Å, while the distance range for stronger vdW is 3.1−5.0 Å. Once two atoms are separated by more than 5.0 Å, the vdW interaction becomes very weak. The PCF curves for (H···O) atom pair in DAP-4 are displayed in Figure 2. The hydrogen atom in $C_6H_{14}N_2^{2+}$and NH_4^+ and oxygen atoms in ClO_4^- were labeled as O and H, respectively. From Figure 2, it

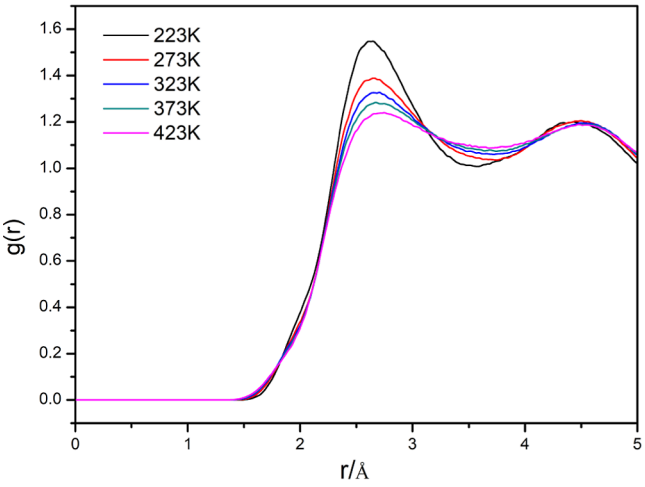

Figure 2. PCF for H···O in the crystal of DAP-4 at different temperatures.

can be found that the PCF curves at different temperatures show relatively high peaks at about 2.4 Å and lower peaks at about 4.6, which suggests that the H···O atom pairs exist in the form of hydrogen bonding in addition to vdw interactions. It can also be seen that the PCF curves slightly shift to the right and its peak height decrease with the increased temperature. This is mainly due to the enhanced atomic motion at elevated temperatures. Thus, it shows that the interaction between atoms decreases with increasing temperature.

3.4. N−H Trigger Bond Length. In the field of energetic compounds, there is a theoretical criterion for judging relative sensitivity.[25] According to the principle of smallest bond order (PBSO), the smaller the bond order of the trigger bond in the chemical structure of a group of energetic compounds, the greater the sensitivity.[26,27] This principle has been applied to predict the impact sensitivity for different kinds of energetic materials. In brief, for a certain type of chemical bond, the longer the bond length, the less stable the bond is, the more likely it is to break during pyrolysis, and the more sensitive the molecule is. Although the electronic structure and bond order data cannot be provided by MD simulation, the statistical data on bond length can be provided by MD simulation in place of the bond order data. Studying the variation of the bond length with temperature can help us to understand the sensitivity of DAP-4 at different temperatures.

https://doi.org/10.1021/acsomega.3c08711
ACS Omega 2024, 9, 4013−4018

According to the studies on the thermal decomposition of DAP-4,[11,12] we can assume that the N−H bond from $C_6H_{14}N_2^{2+}$ and NH_4^+ is the trigger bond of DAP-4. According to the results presented in Table 5, the average bond lengths

Table 5. Trigger Bond (N−H) Lengths (Å) of DAP-4 at Different Temperatures[a]

temperature/K	223	273	323	373	423
L_{ave}	1.003	1.004	1.004	1.005	1.006
	(0.010)	(0.072)	(0.017)	(0.056)	(0.036)
L_{max}	1.144	1.164	1.194	1.211	1.218
	(0.009)	(0.007)	(0.007)	(0.010)	(0.005)

[a]The corresponding deviations for L_{ave} and L_{max} are listed in parentheses.

(L_{ave}) for the trigger bond in the DAP-4 crystal show only a slight enhancement as the temperature rises. However, the maximum bond lengths (L_{max}) exhibit more significant and gradual growth. This suggests that the maximum bond length, rather than the average bond length, is more strongly correlated with the initial bond broken during DAP-4's detonation. As the temperature rises, the maximum bond length gradually rises. For instance, when the temperature reaches 373 K, the maximum bond length adds from 1.144 to 1.211 Å. After reaching this point, the addition in the maximum bond length becomes slower. This indicates that the impact sensitivity of DAP-4 gradually intensifies as the temperature rises. Moreover, when the temperature reaches around 370 K, the impact sensitivity rises at a slower rate with further temperature increments.

3.5. Mechanical Properties. Mechanical properties, as one of the important properties, of high-energetic materials are inextricably related to the preparation, transportation, storage, and usage of high-energetic materials. The elastic modulus of a material, as a measure of its resistance to elastic deformation, is an indication of its stiffness and can also be linked to the plastic and fracture properties of the material. The stiffness and shear strength of a material are indicators of resistance to plastic deformation and are positively correlated with the shear modulus.[28,29] The fracture strength increases with increasing bulk modulus.[30,31] Poisson's ratio (ν) is a measure of the Poisson effect, the deformation (expansion or contraction) of a material in directions perpendicular to the direction of loading. An essential mechanical criterion for determining whether a material is ductile or not is the Pugh's ratio (K/G). The compound is deemed ductile when $K/G > 1.75$; brittle when K/G 1.75. And the larger the K/G value, the better the ductility of the material.[32]

The elastic moduli, Poisson's ratios, and Pugh's ratio K/G of DAP-4 at different temperatures, calculated based on the production trajectory fluctuation analysis and Royce's average values,[33] are presented in Table 6. As can be seen from Table 6, the elastic moduli K, E, and G of the DAP-4 all decrease with increased temperature, thus suggesting that the material's stiffness, hardness, yield strength, and fracture strength all decrease with higher temperature. It is worth noting that Poisson's ratio, which characterizes the lateral deformation of a material under stress, is less affected by temperature variations. Table 6 provides further insights into the relationship between temperature and the compound's properties. The calculated value of K/G, which represents the ratio of the bulk modulus to the shear modulus, augments from 2.22 to 2.53 as the temperature rises until the temperatures surpass 373 K. This indicates that at temperatures below 373 K, the ductility of the compound actually improves with rising temperature. In contrast, at temperatures above 373 K, the ductility of the material tends to decrease as the temperature continues to rise.

4. CONCLUSIONS

In this study, NPT-MD simulations on ammonium perchlorate-based molecular perovskite $(C_6H_{14}N_2)[NH_4(ClO_4)_3]$ were conducted to investigate the effect of temperature on its thermal stability as well as mechanical properties. Cohesive energy density and binding energy calculation for the thermal stability assessment, PCF analysis, the maximum bond length of the N−H trigger bond, and the computation of mechanical properties were all part of the simulations. It is clear from the computed cohesive energy density and binding energies that both of them gradually decrease with temperatures, which means that the interaction among ions weakened, thus demonstrating a decrease in the thermodynamic stability of the system. From the decomposition of CED and E_{bind}, it also can be found that the electrostatic interactions play a crucial part in the molecular interactions. PCF analysis of atom pairs shows that there exists hydrogen bond interaction between H···O atom pairs. The findings in this study suggest that the impact sensitivity of DAP-4, as indicated by the maximum bond length of the N−H trigger bond, gradually rises with higher temperatures. However, this development becomes slower at temperatures above 373 K. Additionally, the mechanical properties of DAP-4, including the moduli (E, K, G), show a consistent decrease as the temperature rises. The ratio of bulk modulus to shear modulus (K/G) grows with temperature, reaching its maximum value at 373 K, and subsequently decreases with further temperature increments. This implies that the material's stiffness, hardness, yield strength, and fracture strength all decline with increasing temperatures. The ductility of the material exhibits an upward trend with rising temperature, reaching its peak at 373 K and then declining as the temperature continues to rise. To sum up, this study provides valuable theoretical insights into the

Table 6. Tensile Modulus (E), Poisson's Ratio (ν), Bulk Modulus (K), Shear Modulus (G), and Quotient K/G at Different Temperatures[a]

parameter	223 K	273 K	323 K	373 K	423 K
K	7.65(0.09)	5.62(0.12)	4.72(0.06)	2.85(0.04)	2.55(0.05)
E	8.99(0.13)	6.08(0.02)	5.02(0.04)	2.98(0.04)	2.95(0.03)
G	3.45(0.05)	2.30(0.03)	1.90(0.02)	1.13(0.04)	1.13(0.06)
ν	0.30(0.00)	0.32(0.00)	0.32(0.00)	0.33(0.00)	0.31(0.00)
K/G	2.22(0.01)	2.44(0.02)	2.49(0.02)	2.53(0.02)	2.26(0.03)

[a]The corresponding deviations are given in brackets. The unit for E, K, and G is GPa.

https://doi.org/10.1021/acsomega.3c08711
ACS Omega 2024, 9, 4013−4018

thermal behavior of molecular perovskite energetic materials, which in turn promotes the process of practical application of energetic molecular perovskite DAP-4.

AUTHOR INFORMATION

Corresponding Author

Jijun Xiao − *Molecules and Materials Computation Institute, School of Chemistry and Chemical Engineering, Nanjing University of Science and Technology, Nanjing 210094, P. R. China*; orcid.org/0000-0003-0054-7957; Email: xiao_jijun@njust.edu.cn

Authors

Qiaoli Li − *Molecules and Materials Computation Institute, School of Chemistry and Chemical Engineering, Nanjing University of Science and Technology, Nanjing 210094, P. R. China*

Shenshen Li − *Molecules and Materials Computation Institute, School of Chemistry and Chemical Engineering, Nanjing University of Science and Technology, Nanjing 210094, P. R. China*

Complete contact information is available at: https://pubs.acs.org/10.1021/acsomega.3c08711

Author Contributions

†Q.L.L. and S.S.L. contributed equally to this work.

Notes

The authors declare no competing financial interest.

ACKNOWLEDGMENTS

This work was funded by the grant from the National Natural Science Foundation of China (grant no. 11572160).

REFERENCES

(1) Suresh Kumar, N.; Chandra Babu Naidu, K. A review on perovskite solar cells (PSCs), materials and applications. *J Mater* **2021**, *7* (5), 940−956.

(2) Abdel, D.; Vágner, P.; Fuhrmann, J.; Farrell, P. Modelling charge transport in perovskite solar cells: Potential-based and limiting ion depletion. *Electrochim. Acta* **2021**, *390*, 138696.

(3) Ye, H. Y.; Tang, Y. Y.; Li, P. F.; Liao, W. Q.; Gao, J. X.; Hua, X. N.; Cai, H.; Shi, P. P.; You, Y. M.; Xiong, R. G. Metal-free three-dimensional perovskite ferroelectrics. *Science* **2018**, *361* (6398), 151−155.

(4) Qarony, W.; Kozawa, M.; Khan, H. A.; Hossain, M. I.; Salleo, A.; Tsang, Y. H.; Hardeberg, J. Y.; Fujiwara, H.; Knipp, D. Vertically Stacked Perovskite Detectors for Color Sensing and Color Vision. *Adv. Mater. Interfaces* **2020**, *7* (17), 2000459.

(5) Chen, S. L.; Yang, Z. R.; Wang, B. J.; Shang, Y.; Sun, L.-Y.; He, C. T.; Zhou, H. L.; Zhang, W. X.; Chen, X. M. Molecular perovskite high-energetic materials. *Sci. China Mater.* **2018**, *61* (8), 1123−1128.

(6) Chen, S. L.; Shang, Y.; He, C. T.; Sun, L. Y.; Ye, Z. M.; Zhang, W. X.; Chen, X. M. Optimizing the oxygen balance by changing the A-site cations in molecular perovskite high-energetic materials. *CrystEngComm* **2018**, *20* (46), 7458−7463.

(7) Shang, Y.; Huang, R. K.; Chen, S. L.; He, C. T.; Yu, Z. H.; Ye, Z. M.; Zhang, W. X.; Chen, X. M. Metal-Free Molecular Perovskite High-Energetic Materials. *Cryst. Growth Des.* **2020**, *20* (3), 1891−1897.

(8) Shang, Y.; Yu, Z. H.; Huang, R. K.; Chen, S. L.; Liu, D. X.; Chen, X. X.; Zhang, W. X.; Chen, X. M. Metal-Free Hexagonal Perovskite High-Energetic Materials with $NH_3OH^+/NH_2NH_3^+$ as B-Site Cations. *Engineering* **2020**, *6* (9), 1013−1018.

(9) Zhang, W. X.; Chen, S. L.; Shang, Y.; Yu, Z. H.; Chen, X. M. Molecular perovskites as a new platform for designing advanced multi-component energetic crystals. *Energ. Mater. Front.* **2020**, *1* (3−4), 123−135.

(10) Boldyrev, V. V. Thermal decomposition of ammonium perchlorate. *Thermochim. Acta* **2006**, *443* (1), 1−36.

(11) Zhou, J.; Ding, L.; Zhao, F.; Wang, B.; Zhang, J. Thermal studies of novel molecular perovskite energetic material $(C_6H_{14}N_2)$-$[NH_4(ClO_4)_3]$. *Chin. Chem. Lett.* **2020**, *31* (2), 554−558.

(12) Deng, P.; Wang, H. X.; Yang, X. B.; Ren, H.; Jiao, Q. J. Thermal decomposition and combustion performance of high-energy ammonium perchlorate-based molecular perovskite. *J. Alloys Compd.* **2020**, *827*, 154257.

(13) Deng, P.; Ren, H.; Jiao, Q. J. Enhanced the combustion performances of ammonium perchlorate-based energetic molecular perovskite using functionalized graphene. *Vacuum* **2019**, *169*, 108882.

(14) Li, X. X.; Hu, S. Q.; Cao, X.; Hu, L. S.; Deng, P.; Xie, Z. B. Ammonium perchlorate-based molecular perovskite energetic materials: preparation, characterization, and thermal catalysis performance with MoS2. *J. Energ. Mater.* **2020**, *38* (2), 162−169.

(15) Liu, Y.; Hu, L. S.; Gong, S. D.; Guang, C. Y.; Li, L. Q.; Hu, S. Q.; Deng, P. Study of Ammonium Perchlorate-based Molecular Perovskite $(H_2DABCO)[NH_4(ClO_4)_3]$/Graphene Energetic Composite with Insensitive Performance. *Cent. Eur. J. Energetic Mater.* **2020**, *17* (3), 451−469.

(16) Zhu, S. D.; Cao, X.; Cao, X. Q.; Feng, Y. Q.; Lin, X. B.; Han, K. H.; Li, X. X.; Deng, P. Metal-doped (Fe, Nd, Ce, Zr, U) graphitic carbon nitride catalysts enhance thermal decomposition of ammonium perchlorate-based molecular perovskite. *Mater. Des.* **2021**, *199*, 109426.

(17) Han, K. H.; Zhang, X. M.; Deng, P.; Jiao, Q. J.; Chu, E. Y. Study of the thermal catalysis decomposition of ammonium perchlorate-based molecular perovskite with titanium carbide MXene. *Vacuum* **2020**, *180*, 109572.

(18) Zhu, W.; Wang, X.; Xiao, J.; Zhu, W.; Sun, H.; Xiao, H. Molecular dynamics simulations of AP/HMX composite with a modified force field. *J. Hazard. Mater.* **2009**, *167* (1−3), 810−816.

(19) Andersen, H. C. Molecular dynamics simulations at constant pressure and/or temperature. *J. Chem. Phys.* **1980**, *72* (4), 2384−2393.

(20) Parrinello, M.; Rahman, A. Polymorphic transitions in single crystals: A new molecular dynamics method. *J. Appl. Phys.* **1981**, *52* (12), 7182−7190.

(21) Allen, M. P.; Tildesley, D. J. Computer Simulation of Liquids. Oxford University Press: England, 1989.

(22) Ewald, P. P. Evaluation of optical and electrostatic lattice potentials. *Ann. Phys.* **1921**, *64*, 253−287.

(23) Sun, T.; Xiao, J. J.; Ji, G. F.; Zhao, F.; Xiao, H. M. Molecular Dynamics Simulation Studies of the CL-20/DNB Co-crystal. *Cent. Eur. J. Energetic Mater.* **2016**, *13*, 677−693.

(24) Li, S. S.; Xiao, J. J. Molecular Dynamics Simulations for Effects of Fluoropolymer Binder Content in CL-20/TNT Based Polymer-Bonded Explosives. *Molecules* **2021**, *26* (16), 4876.

(25) Xiao, J. J.; Wang, W. R.; Chen, J.; Ji, G. F.; Zhu, W.; Xiao, H. M. Study on structure, sensitivity and mechanical properties of HMX and HMX-based PBXs with molecular dynamics simulation. *Comput. Theor. Chem.* **2012**, *999*, 21−27.

(26) Xiao, J. J.; Zhao, L.; Zhu, W.; Chen, J.; Ji, G. F.; Zhao, F.; Wu, Q.; Xiao, H. M. Molecular dynamics study on the relationships of modeling, structural and energy properties with sensitivity for RDX-based PBXs. *Sci. China Chem.* **2012**, *55* (12), 2587−2594.

(27) Xiao, H. M.; Wang, Z. X.; Yao, J. M. Quantum Chemical Study on Sensitivity and Stability of Aromatic Nitro Explosives I. Nitro Derivatives of Aminobenzenes. *Acta Chim. Sin.* **1985**, *43*, 14−18.

(28) Sun, T.; Xiao, J. J.; Liu, Q.; Zhao, F.; Xiao, H. M. Comparative study on structure, energetic and mechanical properties of a ε-CL-20/HMX cocrystal and its composite with molecular dynamics simulation. *J. Mater. Chem. A* **2014**, *2* (34), 13898.

(29) Hu, Q.; Yang, R. Mechanical properties of structural materials from first-principles. *Curr. Opin. Solid State Mater. Sci* **2006**, *10* (1), 19−25.

(30) Xu, X.; Xiao, J.; Huang, H.; Li, J.; Xiao, H. Molecular dynamic simulations on the structures and properties of ε-CL-20(001)/F2314 PBX. *J. Hazard. Mater.* **2010**, *175* (1−3), 423−428.
(31) Xiao, Y. Q.; Sun, T.; Li, S. S.; Xiao, J. J. Molecular Dynamics Simulation Studies of the CL-20/DNB Co-crystal Based PBX with HTPB. *J. Phys.: Conf. Ser.* **2021**, *1721* (1), 012010.
(32) Pugh, S. F. XCII. Relations between the elastic moduli and the plastic properties of polycrystalline pure metals. *Philos. Mag.* **2009**, *45* (367), 823−843.
(33) Parrinello, M.; Rahman, A. Strain fluctuations and elastic constants. *J. Chem. Phys.* **1982**, *76* (5), 2662−2666.

https://doi.org/10.1021/acsomega.3c08711
ACS Omega 2024, 9, 4013−4018